European Radiology (2019) 29:5844–5851
https://doi.org/10.1007/s00330-019-06081-3

MAGNETIC RESONANCE

Radial MP2RAGE sequence for rapid 3D T_1 mapping of mouse abdomen: application to hepatic metastases

Thibaut L. Faller[1] · Aurélien J. Trotier[1] · Sylvain Miraux[1] · Emeline J. Ribot[1]

Received: 28 August 2018 / Revised: 22 January 2019 / Accepted: 7 February 2019 / Published online: 19 March 2019

Abstract

Objectives The T_1 longitudinal recovery time is regarded as a biomarker of cancer treatment efficiency. In this scope, the Magnetization Prepared 2 RApid Gradient Echo (MP2RAGE) sequence relevantly complies with fast 3D T_1 mapping. Nevertheless, with its Cartesian encoding scheme, it is very sensitive to respiratory motion. Consequently, a radial encoding scheme was implemented for the detection and T_1 measurement of hepatic metastases in mice at 7T.

Methods A 3D radial encoding scheme was developed using a golden angle distribution for the k-space trajectories. As in that case, each projection contributes to the image contrast, the signal equations had to be modified. Phantoms containing increasing gadoteridol concentrations were used to determine the accuracy of the sequence in vitro. Healthy mice were repetitively scanned to assess the reproducibility of the T_1 values. The growth of hepatic metastases was monitored. Undersampling robustness was also evaluated.

Results The accuracy of the T_1 values obtained with the radial MP2RAGE sequence was > 90% compared to the Inversion-Recovery sequence. The motion robustness of this new sequence also enabled repeatable T_1 measurements on abdominal organs. Hepatic metastases of less than 1-mm diameter were easily detected and T_1 heterogeneities within the metastasis and between the metastases within the same animal were measured. With a twofold acceleration factor using undersampling, high-quality 3D T_1 abdominal maps were achieved in 9 min.

Conclusions The radial MP2RAGE sequence could be used for fast 3D T_1 mapping, to detect and characterize metastases in regions subjected to respiratory motion.

Key Points

- *The Cartesian encoding of the MP2RAGE sequence was modified to a radial encoding. The modified sequence enabled accurate T_1 measurements on phantoms and on abdominal organs of mice.*
- *Hepatic metastases were easily detected due to high contrast. Heterogeneity in T_1 was measured within the metastases and between each metastasis within the same animal.*
- *As implementation of this sequence does not require specific hardware, we expect that it could be readily available for clinical practice in humans.*

Keywords Magnetic resonance imaging · Mice · Three-dimensional imaging · Liver · Metastasis

Abbreviations

bSSFP	Balanced steady-state free precession
MP2RAGE	Magnetization Prepared 2 RApid Gradient Echoes

Introduction

Metastases are one of the major causes of mortality in cancer, due to their whole-body spread. MRI is a technique of choice for oncology due to high soft tissue contrasts and the absence of radiation. Nevertheless, to monitor tumors under treatment, a

Electronic supplementary material The online version of this article (https://doi.org/10.1007/s00330-019-06081-3) contains supplementary material, which is available to authorized users.

✉ Emeline J. Ribot
ribot@rmsb.u-bordeaux.fr

[1] Centre de Résonance Magnétique des Systèmes Biologiques, UMR 5536, CNRS/University Bordeaux, 146 rue Léo Saignat, 33076 Bordeaux, France

longitudinal quantitative approach would be an additional asset. The T_1 spin-lattice relaxation time has been shown to be a biomarker of a cancer therapy response in mice [1, 2]. In order to accurately measure T_1 in metastases at an early stage, when their volumes are small, it is crucial to get 3D MR images with high spatial resolution, especially for preclinical studies.

3D T_1 mapping sequences have already been developed for rat and mouse brains at high magnetic fields [3, 4]. However, obtaining T_1 maps of the abdomen of small animals is still challenging mainly due to respiratory motion that deteriorates the quality of 3D high-resolution images. A way of reducing such artifacts is to synchronize the acquisition with the animal respiration; still, respiration triggering is time-consuming and may not be suitable for T_1 measurement. Contrary to Cartesian encoding scheme, radial encoding is much less sensitive to motion because of the repetitive k-space center acquisition in different directions [5]. In addition, because of the low frequencies over-sampling, high signal-to-noise ratio (SNR) can thus be obtained, and images can be acquired more rapidly with only a few projections. Motion impacted projections can also be removed a posteriori using a self-gating algorithm.

On small animals, radial sampling encoded T_1 mapping sequences based on the inversion [6] or saturation [7, 8] recovery approaches are generally employed to obtain 2D maps. A 3D Look-Locker sequence, using a stack-of-spiral encoding scheme, has also been developed for mouse heart and brain imaging [4, 9]. Yet, its application to abdominal imaging may be challenging due to off-resonance effects caused by the high fat content in the abdomen [10].

Variable flip angle (VFA)–based sequences were applied in 3D on the mouse heart in vivo [11]. However, this technique seems to measure T_1 with low accuracy [12].

An alternative method for T_1 mapping is the Cartesian encoded Magnetization Prepared 2 RApid Gradient Echoes (MP2RAGE) sequence [13]. It leads to the fast acquisition of 3D T_1 maps (less than 15 min for 1-mm isotropic human brain map) with good accuracy.

This sequence has been used in neuroimaging for its high T_1 contrasts at magnetic fields higher than 1.5T. It has been used on humans [14–16] and on small animals at 7T in combination with the Compressed Sensing technique [17], 9.4T and 14.1T to obtain brain T_1 maps in the presence of manganese [18].

Consequently, the goal of our study was to develop a 3D radial MP2RAGE sequence and consequently to assess 3D T_1 maps of the mouse abdomen at 7T. The influence of the radial encoding scheme on motion sensitivity and T_1 accuracy was evaluated. This sequence was then applied to detect and characterize hepatic metastases in mice at 7T. In the aim of reducing acquisition time, the effect of undersampling was studied.

Materials and methods

MRI system

Experiments were performed on a 7T Bruker BioSpec system equipped with a gradient coil of 660 mT m^{-1} maximum strength and 110 μs rise time.

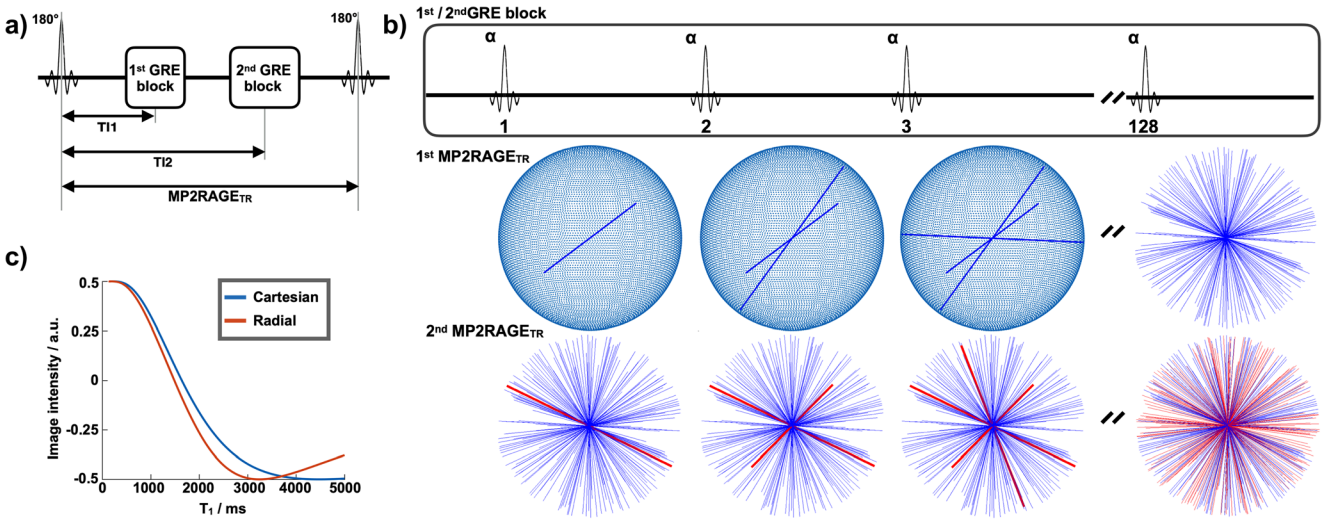

Fig. 1 Description of the 3D pseudo random radial encoded MP2RAGE sequence. **a** An inversion pulse (180°) is followed by two GRadient Echo blocks (GRE block), containing *n* pulses. The inversion times (TI) correspond to the time between the middle of the inversion pulse (180°) and the middle of the GRE block (*n/2th* pulse). $MP2RAGE_{TR}$ corresponds to the time between two inversion pulses. **b** In our case, a total of 128 echoes were read to acquire 128 k-space diameters. These diameters were reordered using a pseudo golden ratio (as shown for one GRE block in dark blue). During one $MP2RAGE_{TR}$, both echo blocks acquire the same k-space diameters. At the next $MP2RAGE_{TR}$, another set of diameters are acquired (shown in red); the first diameter of this set being the successor (in the pseudo random sequence) of the 128th echo of the previous $MP2RAGE_{TR}$. **c** Corresponding radial (red) and standard Cartesian (blue) MP2RAGE lookup-tables are shown

A volume resonator operating in quadrature mode was used for excitation (75.4-mm inner diameter, 70-mm active length), and a proton phased array (RAPID Biomedical GmbH) was used for signal reception (4 elements of 30 mm long around an elliptic cylinder housing: 19 × 25.5 mm).

3D pseudo random radial encoded MP2RAGE sequence

Figure 1a) presents a simplified diagram of the MP2RAGE sequence [16]. Its Cartesian k-space sampling scheme was replaced by a radial one. After each of the 128 inversions, two gradient echo (GRE) blocks of 128 projections each were acquired at two inversion times (TI). The sequence was repeated 128 times, with a delay ($MP2RAGE_{TR}$) between two inversions. The whole set of projections was acquired in a quasi-golden ratio order using the same distribution as Koktzoglou et al [19]. Figure 1b) illustrates this encoding scheme by displaying the 1st, 2nd, 3rd, and the 128 projections registered during a GRE block acquired during the first two $MP2RAGE_{TR}$.

Radial MP2RAGE signal equations

As in [13], two images could be reconstructed from respectively all first and second GRE blocks, and combined to obtain a "MP2RAGE" image, where the signal only depends on the T_1 and sequence parameters but not on B_1^+ and T_2*.

In the Cartesian case, the signal is assumed to come only from the central echo of each GRE block (*n/2* in ref. [13]). This assumption does not hold for a radial encoding scheme: as the signal of the k-space center is acquired at each echo, all the *n* echoes of one GRE block influence the image intensity. Therefore, to get closer to the specificity of the radial MP2RAGE sequence, the image signal was simulated using the average signal of the *n* echoes of a GRE block. Therefore, the signal equations were modified accordingly by replacing *n/2* by $m \in [1;n]$ (Supplementary material 1) and a new look-up table was generated.

As shown in Fig. 1c), in the T_1 range of 800–2000 ms, for the same T_1 values, the MP2RAGE signal intensity is lower in the radial case than in the Cartesian one.

Phantom imaging

Five tubes containing physiological serum and gadoteridol (ProHance®, Bracco imaging) at different concentrations were prepared to obtain T_1 values from 800 to 2000 ms.

The T_1 values were determined via the gold standard Inversion-Recovery (IR) sequence: 120 TI from 100 to 12,000 ms (100 ms increment), echo time (TE) = 10 ms, repetition time (TR) = 15 s, field of view (FOV) 25 × 18 mm^2, matrix = 128 × 64, resolution 195 × 281 μm^2, 1 slice, thickness = 2 mm, scan time ≈ 8 h.

Then, the Cartesian and radial MP2RAGE sequences were performed: inversion pulse (180° adiabatic hyperbolic secant pulse of 10 ms), TI_1-TI_2-$MP2RAGE_{TR}$ = 1000–3300–8250 ms (as recommended at 7T [13]), 1 ms sinc 10 lobes pulses, $\alpha 1 = \alpha 2 = 7°$, Inter-echo repetition time (TR) 7 ms, echo time TE = 3.2 ms (Cartesian) or 2.7 ms (radial), FOV = $(25\ mm)^3$, matrix = $(128)^3$, resolution = $(195\ \mu m)^3$, reception bandwidth (rBW) = 391 Hz/pixel, scan time = 18 min. For all radial acquisitions, the same trajectories required for the regridding process were used. The scans were averaged ten times on a phantom filled with water to correct both eddy current and gradient delay errors [20].

All three acquisitions (IR and both MP2RAGE sequences) were performed five times and the MP2RAGE measurements were compared to the IR measurements.

In vivo imaging

Animal preparation

C57/Bl6 mice (8 weeks old, Charles River) were used in this study.

A first group ($N = 8$) was dedicated to brain imaging.

A second group ($N = 3$, called "healthy mice" thereafter) was used for abdominal imaging.

A last group ($N = 6$) received a mesenteric injection of 2×10^5 B16F10 murine melanoma cells in 100 μL DMEM, as previously described [21]. Briefly, a small incision was made along the midline of the low abdomen to expose the intestines. The mesenteric vein was used to inject the cancer cells.

A self-gated Cartesian balanced steady-state free precession (bSSFP) experiment was used to assess the presence of metastases: TE/TR = 2/4 ms, flip angle: 30° hermite pulse, rBW = 781.25 Hz/pixel. The FOV and resolution were the same as the MP2RAGE ones, with 5 self-gating points per line, 4 images with frequency offsets = 0, 61, 122, and 183 Hz, and 4 repetitions each resulting in a total acquisition time of 17 min 28 s. The self-gated images were reconstructed as in [22].

All experimental procedures were approved by the Animal Care and Use Institutional ethics committee of Bordeaux, France (approval no. 5012032-A).

In vivo MRI

Brain and abdomen T_1 maps were acquired with the MP2RAGE sequences. The mice were positioned in the coil in such a manner that either the brain or both the kidneys and the liver were observable. The mice were anesthetized with isoflurane (1–2% in air). The respiration was monitored using a balloon placed on the lower abdomen (SA Instruments). The same imaging parameters as for the in vitro experiments were used.

Each healthy mouse was scanned three times at three different days. The hepatic metastases-bearing mice were scanned at days 11, 13, 15, 18, and 22 post-injection.

Image analysis

After acquisition, T_1 maps were reconstructed and analyzed using Matlab® software (Mathworks).

Regions of interest (ROI) were drawn on each phantom tube on the T_1 maps obtained with the MP2RAGE sequences. Their T_1 values were also measured from the IR sequence through an exponential curve fitting. The mean T_1 was measured as an average of the T_1 values of each voxel within a ROI.

To compare MP2RAGE T_1 measurements in vivo in a region not subject to respiratory motion and obtained with the Cartesian and the radial MP2RAGE sequences, ROIs were manually drawn on a single slice of the T_1 maps in the head muscle, brain cortex, and midbrain (Supplementary Material 3). On the abdominal radial T_1 maps, the reproducibility of the measurements was evaluated through ROIs drawn in the healthy liver, and on three areas of the kidneys (cortex, inner medulla, and outer medulla) and in the hepatic metastases ($N = 20$). The mean T_1 was measured as a mean of the T_1 values of each voxel within a ROI.

To compare the homogeneity of the Cartesian and radial T_1 maps, a ROI void of main blood vessels was drawn. The number of pixels as a function of the T_1 values was represented with histograms. The full width at half maximum (FWHM) [22] was measured.

To measure the volume of a metastasis over time, segmentation was performed on the T_1 maps using Amira® software (TGS).

To assess the impact of undersampling on the quality of the abdominal MP2RAGE images, T_1 maps were reconstructed with only half, quarter, or eighth of the dataset (corresponding to 8192, 4096, and 2048 projections, respectively), to simulate acquisition times of 9, 4.5, and 2.5 min. As the projections were arranged in a pseudo random way, this truncation affected the whole image isotropically.

Then, difference images were generated by subtracting the original T_1 map from the three undersampled T_1 maps.

Statistics

Statistically significant differences between in vitro measurements (5 different tubes, 5 independent experiments) were analyzed by the one-way ANOVA test followed by the Bonferroni post-test using Graphpad Prism 5.0® software. A p value lower than 0.05 was considered to be statistically significant.

After checking the normal distribution of the data (Shapiro-Wilk test, $N = 5$, alpha = 0.05), the TOST equivalence test was also performed [23] to evaluate the equivalence of the T_1 mapping methods (delta = 0, alpha = beta = 0.05). The confidence intervals for the differences in mean values (Eq. 8 in [23]) were calculated for both sequences as well as the maximum mean difference for each measurement (⊖).

Results

In vitro T_1 measurement accuracy

The T_1 value obtained from the multiple concentrations of gadolinium were similar between the Cartesian and the radial MP2RAGE sequences and showed no significant difference with the IR sequence. The TOST test revealed a difference smaller than 10% between the measurements obtained with the Inversion-Recovery and both MP2RAGE sequences (Supplementary material 2).

In vivo brain imaging

3D T_1 maps were first acquired on the brain of healthy mice using both MP2RAGE sequences (Supplementary material 3). The T_1 values of several brain structures had small standard deviations, showing a high repeatability of both sequences. The differences in T_1 measurements between the Cartesian and the radial sequences were minor compared to the T_1 values (< 6%).

Robustness to respiratory motion

Figure 2a shows mouse abdominal images (TI_1, TI_2, and MP2RAGE images in addition to the T_1 maps) acquired with the Cartesian and the radial MP2RAGE sequences. The background of the radial images looks slightly noisy due to the shape of the point-spread function [5]. However, on the radial TI_1 and TI_2 images, a better spatial homogeneity of the liver signal is observed leading to an approximately 50% drop in the FWHM on the T_1 map (Fig. 2b).

As a result, an easy detection of hepatic blood vessels on the radial maps (arrow) was possible, as compared to the Cartesian ones (magnified T_1 maps).

In vivo T_1 measurement reproducibility on the healthy abdomen

As shown in Fig. 3, the T_1 measured in the liver and in the kidneys with the radial sequence are similar between mice and throughout each day of acquisition. The mean T_1 of the liver and the cortex, outer medulla and inner medulla of the kidney were found to be 1133 ± 34 ms, 1309 ± 57 ms, 1740 ± 62 ms, and 2677 ± 162 ms, respectively. In the liver, the standard deviations for the three mice were 34, 34, and 28 ms respectively.

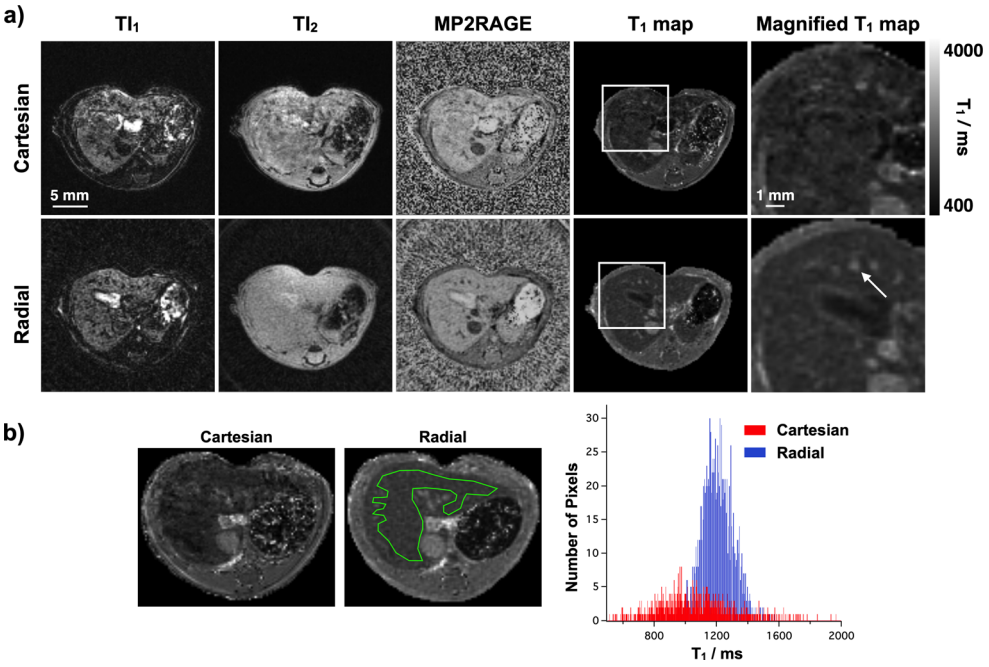

Fig. 2 **a** Axial views of mouse abdominal images obtained at the first (TI_1) and second (TI_2) GRE blocks, their combination (MP2RAGE) and the corresponding T_1 maps. The images were acquired with the Cartesian (first row) and radial (low row) sequences. The arrow underlines the improved homogeneity of the liver on the radial images, which enables to easily detect small hepatic blood vessels. **b** Histogram representing the number of pixels per T_1 values from the region of interest (green line) applied on both axial T_1 maps

Metastasis detection and characterization

Hepatic metastases as small as 0.2 mm^3 (representing approximately 25 voxels) could be detected prospectively on the radial MP2RAGE T_1 map due to their T_1 longer than the surrounding tissues (Fig. 4). The mean T_1 of all the metastases analyzed was 1800 ± 200 ms. Their presence was confirmed by a self-gated bSSFP sequence [22].

Throughout the longitudinal study, the bSSFP sequence showed an increasing heterogeneity of the signal inside the metastases. The corresponding T_1 maps show that this is partially caused by T_1 heterogeneities.

For instance, at day 22, a representative metastasis shown in Fig. 4 had areas with long T_1 (> 1800 ms), medium T_1 (between 1400 and 1800 ms), and short T_1 (≈ 1000 ms).

Histology was also performed on this metastasis mouse model and demonstrated that long T_1 within metastases could correspond to the presence of edema (Supplementary Material 4).

Undersampling effect

In order to decrease acquisition time, multiple undersampling factors were tested (Fig. 5). Using only half of the dataset (reducing the duration to 9 min) did not significantly alter

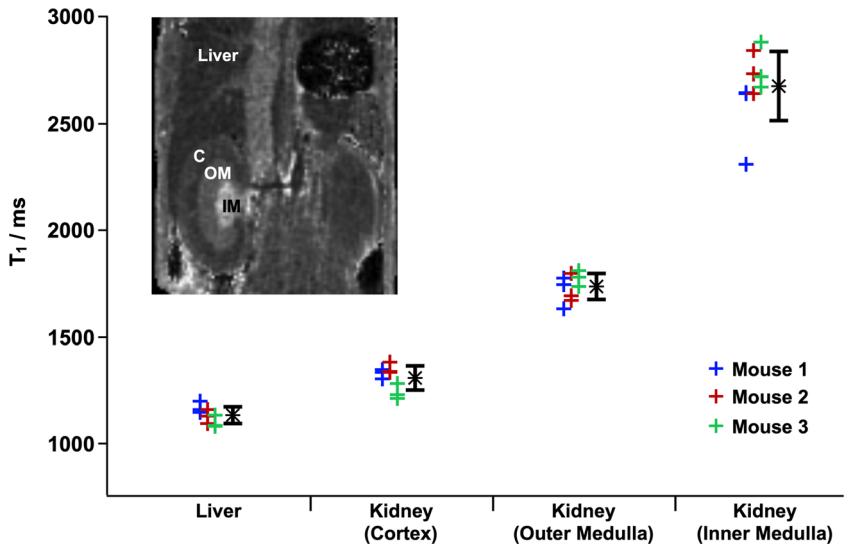

Fig. 3 T_1 measurements of four abdominal regions of healthy mice. T_1 measurements on the liver and the kidney (cortex (C), outer medulla (OM), and inner medulla (IM)) have been performed on three mice (blue, red, and green) on three different days. Global averages and standard deviations are displayed in black. The magnification of a MP2RAGE T_1 map shows the three kidney regions. The standard deviations of the liver T_1 over the three days were 34, 34, and 28 ms for the "blue", "red," and "green" mice, respectively

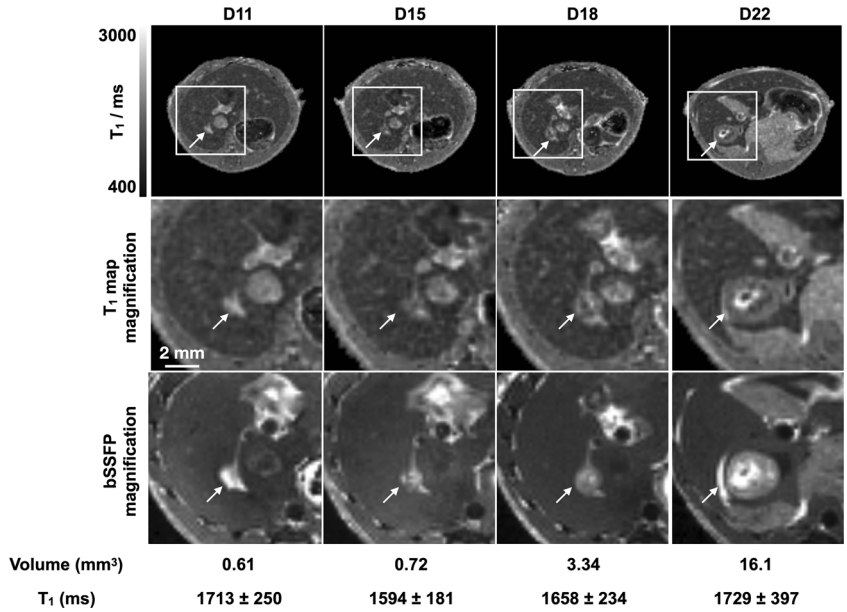

Fig. 4 Longitudinal follow up of a mouse hepatic metastasis (arrows). First row: axial views of T_1 maps acquired with the radial MP2RAGE sequence at days 11, 15, 18, and 22 post-injection. Second row: magnification of the T_1 maps. Third row: corresponding magnifications from the bSSFP images. The metastasis volume and mean T_1 are indicated below

the quality of the T_1 map. Indeed, the difference map remained homogeneous, particularly in the liver. Using fourth of the dataset, some hepatic blood vessels were no longer detectable for example (plain arrow), but a metastasis of 1-mm diameter could be easily identified; its detection got altered only when the undersampling factor was set to 8. In parallel, the difference maps were getting more heterogeneous in the liver region. Yet, reducing the number of projections used for the reconstruction did not globally alter the T_1 measurements of a large ROI in the liver.

Discussion

In this work, the Cartesian encoding scheme of the MP2RAGE sequence was replaced by a radial scheme for respiratory motion–related artifact robustness. Without respiration synchronization, 3D T_1 maps of the mouse abdomen were generated with an isotropic resolution of 0.2 mm within 18 min. Using an adequate look-up table, the sequence was shown to be accurate in vitro, and repeatable in vivo. The sequence was therefore used to detect and characterize hepatic metastases. A great variability was observed among metastases, some being quite homogeneous, others containing regions of very long or short T_1, irrespective of their sizes. This is consistent with a previous study that performed diffusion MRI on the same metastasis model [24]. Finally, the image quality was preserved using only half of the projections, resulting in 3D T_1 maps acquired in 9 min.

The T_1 measured in the brain cortex at 7T was approximately 150 ms shorter than the one obtained using a 2D Cartesian Look-Locker sequence [25], but 200 ms longer than

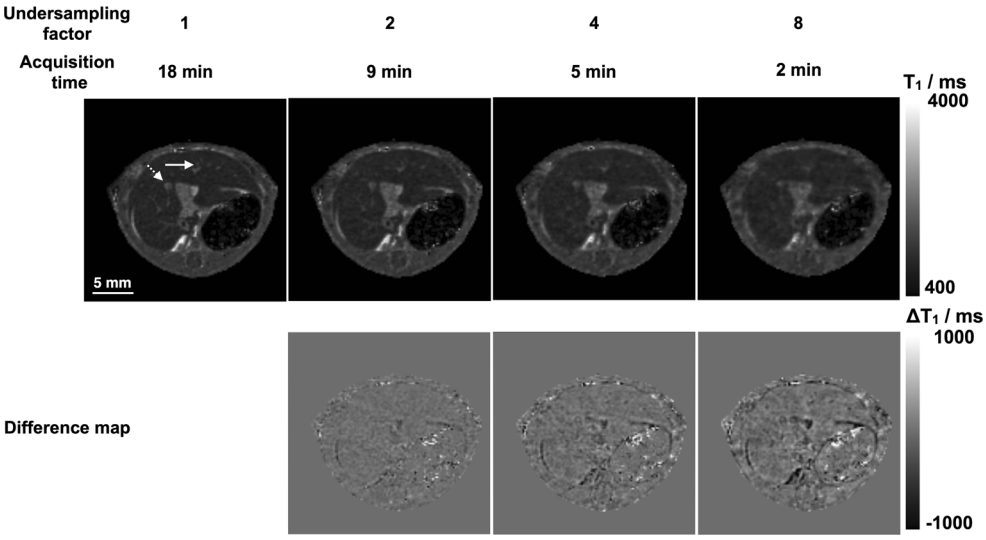

Fig. 5 Effect of undersampling on radial 3D T_1 maps of mouse abdomen. The first row shows the axial views of T_1 maps reconstructed using undersampling factors of 1, 2, 4, and 8. The second row shows the difference between the undersampled images and the initial T_1 map

those reported in Swiss nu/nu mice using a 3D Look-Locker sequence [4]. Also, the T_1 measurements in the liver were 140 ms longer than the one obtained using a 2D Spin-Echo Cartesian sequence. The high variability of T_1 measurements within the literature is also highlighted by Lee et al [26], where T_1 measured in the kidney cortex using a 2D variable TR Turbo Spin-Echo sequence was found to vary from 1346 ± 175 to 1892 ± 209 ms depending on the slice position.

Some differences might also come from the 2D versus 3D encodings. Indeed, 2D sequences require large slice thickness, which can contain different structures within the same voxel and consequently will influence the T_1 value measurements. In addition, the absence of respiration triggering can affect the T_1 measurements obtained with Cartesian sequences. In vivo, because of magnetization transfer, magnetization recovery is better described by a bi-exponential curve [27]. The hypothesis of a mono-exponential magnetization recovery model could therefore influence the T_1 measurements. Sequences using curve fitting reconstruction algorithms as Look-Locker or the MPnRAGE sequence [28] might be able to more precisely evaluate this recovery scheme in small animals. In our case, the radial MP2RAGE sequence was considered the best compromise between T_1 accuracy, acquisition time, and 3D spatial resolution.

One limitation of the sequence, except the requirement of trajectory measurements inherent to non-Cartesian imaging, is the hypothesis of a constant and ideal transmit B_1 field. However, simulations showed that an overestimation of 10% of the transmit B_1 field could lead to T_1 over-estimations below 2%.

In our study, the motion-affected projections were not deleted, as the quality of the images was high enough to detect small metastases. Nevertheless, due to the robustness to undersampling of the sequence, the self-gating method could be advantageous especially for human imaging, where a large part of the projections may be altered by respiration motion. This technique has been demonstrated efficient in mice even when a steady state is not reached [8].

To allow T_1 mapping of large cohorts of animals or to shorten anesthesia duration, a further reduction of acquisition duration would be needed. This could be obtained by increasing the number of echoes per GRE block, probably at the expense of some T_1 accuracy. Strategies like Compressed Sensing (CS) or parallel imaging could also be used. Both have already been combined to accelerate radial 2D acquisitions [29, 30] and 3D Cartesian parametric maps [31, 32]. In addition, parallel imaging [33] and CS [17] have been independently combined with the Cartesian MP2RAGE sequence enabling to obtain human and mouse brain T_1 maps, in less than 6 min. Both techniques will be necessary to acquire human abdominal T_1 maps with reasonable spatial resolution (3–5 mm isotropic) in less than 20 min using a standard clinical MR system.

In conclusion, through the modification of its encoding scheme, the MP2RAGE sequence is becoming relevant to map other regions than the brain. Indeed, its motion robustness is now sufficient to detect small metastasis in regions impacted by respiratory motion. Hence, it enables the fast acquisition of 3D T_1 maps using a standard preclinical system (magnet and gradients). The only prerequisite for T_1 accuracy is a homogenous transmit coil. Then, T_1 can be used as a diagnostic and monitoring biomarker in small animals and could be of high potential for clinical applications. Still, further investigations performed when applying a therapy are needed to confirm this.

Funding This study has received funding by the Laboratory of Excellence TRAIL ANR-10-LABX-57.

Compliance with ethical standards

Guarantor The scientific guarantor of this publication is Emeline J Ribot.

Conflict of interest The authors of this manuscript declare no relationships with any companies, whose products or services may be related to the subject matter of the article.

Statistics and biometry No complex statistical methods were necessary for this paper.

Ethical approval Approval from the Animal Care and Use Institutional ethics committee of Bordeaux was obtained.

Methodology
- prospective
- experimental
- performed at one institution

References

1. Weidensteiner C, Allegrini PR, Sticker-Jantscheff M, Romanet V, Ferretti S, McSheehy PMJ (2014) Tumour T1 changes in vivo are highly predictive of response to chemotherapy and reflect the number of viable tumour cells – a preclinical MR study in mice. BMC Cancer 14:88–100
2. Ravoori MK, Nishimura M, Singh SP, Lu C, Han L (2015) Tumor T1 relaxation time for assessing response to bevacizumab anti-angiogenic therapy in a mouse ovarian cancer model. PLoS One 10:1–13
3. Chuang K-H, Koretsky A (2006) Improved neuronal tract tracing using manganese enhanced magnetic resonance imaging with fast T(1) mapping. Magn Reson Med 55:604–611
4. Castets CR, Koonjoo N, Hertanu A et al (2016) In vivo MEMRI characterization of brain metastases using a 3D Look-Locker T1-mapping sequence. Sci Rep 6:39449–39457
5. Glover GH, Pauly JM (1992) Projection reconstruction techniques for reduction of motion effects in MRI. Magn Reson Med 28:275–289
6. Nezafat M, Ramos IT, Henningsson M, Protti A, Basha T, Botnar R (2017) Improved segmented modified Look-Locker inversion recovery T1 mapping sequence in mice. PLoS One 12:e0187621

7. Messroghli DR, Nordmeyer S, Buehrer M et al (2011) Small animal Look-Locker inversion recovery (SALLI) for simultaneous generation of cardiac T1 maps and cine and inversion recovery-prepared images at high heart rates: initial experience. Radiology 261:258–265
8. Winter P, Kampf T, Helluy X et al (2016) Self-navigation under non-steady-state conditions: cardiac and respiratory self-gating of inversion recovery snapshot FLASH acquisitions in mice. Magn Reson Med 76:1887–1894
9. Castets CR, Ribot EJ, Lefrançois W et al (2015) Fast and robust 3D T_1 mapping using spiral encoding and steady RF excitation at 7T: application to cardiac manganese enhanced MRI (MEMRI) in mice. NMR Biomed 28:881–889
10. Wang D, Zwart NR, Pipe JG (2017) Joint water-fat separation and deblurring for spiral imaging. Magn Reson Med 79:3218–3228
11. Coolen BF, Geelen T, Paulis LEM, Nauerth A, Nicolay K, Strijkers GJ (2011) Three-dimensional T1 mapping of the mouse heart using variable flip angle steady-state MR imaging. NMR Biomed 24:154–162
12. Stikov N, Boudreau M, Levesque IR, Tardif C, Barral K, Pike GB (2015) On the accuracy of T1 mapping: searching for common ground. Magn Reson Med 522:514–522
13. Marques JP, Kober T, Krueger G, van der Zwaag W (2010) NeuroImage MP2RAGE , a self-bias-field corrected sequence for improved segmentation and T1-mapping at high field. Neuroimage 49:1271–1281
14. Næss-Schmidt ET, Tietze A, Mikkelsen IK et al (2015) Patch-based segmentation from MP2RAGE images: comparison to conventional techniques. First International Workshop on Patch-based Techniques in Medical Images (Patch-MI 2015), Oct 2015, Munich, Germany. Patch-Based Techniques in Medical Imaging First International Work- shop, Patch-MI 2015, held in conjunction with MICCAI 2015, Munich, Germany, October 9, 2015, Revised Selected Papers, 9467, pp.180-187, 2016, Lecture Notes in Computer Science. <10.1007/978-3-319-28194-0 22>. <hal-01290510>
15. Fujimoto K, Polimeni JR, van der Kouwe AJW et al (2014) Quantitative comparison of cortical surface reconstructions from MP2RAGE and multi-echo MPRAGE data at 3 and 7T. Neuroimage 90:60–73
16. Marques JP, Gruetter R (2013) New developments and applications of the MP2RAGE sequence - focusing the contrast and high spatial resolution R1 mapping. PLoS One 8:e69294
17. Trotier A, Rappachi S, Faller T, Miraux S, Ribot EJ (2019) Compressed-sensing MP2RAGE sequence: application to the detection of brain metastases in mice at 7T. Magn Reson Med 81:551–559
18. Driencourt L, Romero CJ, Lepore M, Eggenschwiler F, Reynaud O, Just N (2017) T1 mapping of the mouse brain following fractionated manganese administration using MP2RAGE. Brain Struct Funct 222:201–214
19. Koktzoglou I (2013) 4D dark blood arterial wall magnetic resonance imaging: methodology and demonstration in the carotid arteries. Magn Reson Med 69:956–965
20. Beaumont M, Lamalle L, Segebarth C, Barbier EL (2007) Improved k-space trajectory measurement with signal shifting. Magn Reson Med 58(1):200–205
21. Morris VL, MacDonald IC, Koop S, Schmidt EE, Chambers AF, Groom AC (1993) Early interactions of cancer cells with the microvasculature in mouse liver and muscle during hematogenous metastasis: videomicroscopic analysis. Clin Exp Metastasis 11:377–390
22. Ribot EJ, Duriez TJ, Trotier AJ, Thiaudiere E, Franconi JM, Miraux S (2015) Self-gated bSSFP sequences to detect iron-labeled cancer cells and/or metastases in vivo in mouse liver at 7 Tesla. J Magn Reson Imaging 41:1413–1421
23. Limentani GB, Ringo MC, Ye F, Bergquist ML, MacSorley EO (2005) Beyond the t-test: statistical equivalence testing. Anal Chem 77:221–226
24. Ribot EJ, Trotier AJ, Castets CR et al (2016) Free-breathing 3D diffusion MRI for high-resolution hepatic metastasis characterization in small animals. Clin Exp Metastasis 33:167–178
25. Guilfoyle DN, Dyakin VV, O'Shea J, Pell GS, Helpern JA (2003) Quantitative measurements of proton spin-lattice (T1) and spin-spin (T2) relaxation times in the mouse brain at 7.0 T. Magn Reson Med 49:576–580
26. Lee DK, Han S, Cho HJ (2017) Optimization of sparse phase encodings for variable repetition-delay turbo-spin echo (TSE) T1 measurements for preclinical applications. J Magn Reson 274:57–64
27. Rioux JA, Levesque IR, Rutt BK (2016) Biexponential longitudinal relaxation in white matter: characterization and impact on T1 mapping with IR-FSE and MP2RAGE. Magn Reson Med 75:2265–2277
28. Kecskemeti S, Samsonov A, Hurley SA, Dean DC, Field A, Alexander AL (2016) MPnRAGE: a technique to simultaneously acquire hundreds of differently contrasted MPRAGE images with applications to quantitative T1 mapping. Magn Reson Med 75:1040–1053
29. Feng L, Axel L, Chandarana H, Block KT, Sodickson DK, Otazo R (2016) XD-GRASP: golden-angle radial MRI with reconstruction of extra motion-state dimensions using compressed sensing. Magn Reson Med 75:775–788
30. Huang C, Graff CG, Clarkson EW, Bilgin A, Altbach MI (2012) T2 mapping from highly undersampled data by reconstruction of principal component coefficient maps using compressed sensing. Magn Reson Med 67:1355–1366
31. Weingärtner S, Akçakaya M, Roujol S et al (2015) Free-breathing post-contrast three-dimensional T1 mapping: volumetric assessment of myocardial T1 values. Magn Reson Med 73:214–222
32. Bhave S, Lingala SG, Johnson CP, Magnotta VA, Jacob M (2016) Accelerated whole-brain multi-parameter mapping using blind compressed sensing. Magn Reson Med 75:1175–1186
33. Shin W, Shin T, Oh S-H, Lowe MJ (2016) CNR improvement of MP2RAGE from slice encoding directional acceleration. Magn Reson Imaging 34:779–784